Growth and Characterization of BPO_4 Single Crystals

M. Schmidt[a], B. Ewald[a], Yu. Prots[a], R. Cardoso-Gil[a], M. Armbrüster[a], I. Loa[b], L. Zhang[a], Ya-Xi Huang[a], U. Schwarz[a,*], and R. Kniep[a]

[a] Dresden, Max-Planck-Institut für Chemische Physik fester Stoffe, Nöthnitzer Str. 40, 01187 Dresden
[b] Stuttgart, Max-Planck-Institut für Festkörperforschung, Heisenbergstr. 1, 70569 Stuttgart

Received January 12th, 2004.

In memoriam Professor Peter Böttcher

Abstract. Single crystals of BPO_4 were grown by chemical transport reactions with PCl_5 using a gradient from 1073 K to 973 K as well as with solvothermal syntheses in the temperature range between 413 K and 523 K using water, ethanol or 2-propanol as polar protic solvents. The atomic arrangement of BPO_4 was reinvestigated by means of single crystal X-ray diffraction data and confirmed the earlier findings with significantly smaller standard deviations. Thermogravimetric investigations of powdered samples which show no extra lines in X-ray diffraction diagrams revealed weight decrements which are attributed to water losses. The presence of protonated borate and phosphate species in a number of X-ray pure solvothermally grown BPO_4 samples is evidenced by infrared spectroscopy.

Keywords: Boron; BPO_4; Crystal growth; Crystal structure

Kristallzüchtung und Charakterisierung von BPO_4-Einkristallen

Inhaltsübersicht. Einkristalle von BPO_4 wurden durch chemische Transportreaktionen mit PCl_5 in einem Gradienten von 1073 K nach 973 K sowie durch solvothermale Synthesen im Temperaturbereich zwischen 413 K und 523 K mit Wasser, Ethanol oder 2-Propanol als polare protische Solvenzien gezüchtet. Die Anordnung der Atome von BPO_4 wurde erstmalig mit Röntgenbeugungsdaten von Einkristallen verfeinert und bestätigt im wesentlichen die früheren Ergebnisse bei signifikant kleineren Standardabweichungen. Thermogravimetrische Untersuchungen von pulverförmigen Proben, deren Röntgenbeugungsdiagramme keine zusätzlichen Linien erkennen lassen, zeigen Gewichtsverluste, die auf Wasserabgabe zurückgeführt werden. Die Gegenwart protonierter Borat- und Phosphatspezies in einer ganzen Reihe solvothermal gezüchteter BPO_4 Proben kann durch Infrarotspektroskopie nachgewiesen werden.

Introduction

BPO_4 is formed when equimolar amounts of boric and concentrated phosphoric acid are mixed. The compound precipitates as a white residue after boiling and evaporating aqueous solutions [1−5]. The raw products are described as white powders which are soluble in water. They become insoluble and crystalline after heating the precipitate to temperatures between 973 K and 1073 K. The formation of BPO_4 was even suggested to represent a good analytical method for quantitative determinations of the borate concentrations in solution [4, 6, 7]. The formation of possible hydrates of BPO_4 has been investigated by thermal methods [8] but predicted compounds have not been confirmed independently in a more comprehensive fashion.

An initial structural investigation of BPO_4 using small tetragonal-bisphenoidically shaped crystals obtained by heating mixtures of $(NH_4)_2HPO_4$ with excess H_3BO_3 followed by annealing was performed quite early [9] and revealed the tetragonal space group $I\bar{4}$ (No. 82) with a = 434.4 pm, c = 664.3 pm, and Z = 2. Intensity analyses resulted in a structural model revealing that boron and phosphorus are both tetrahedrally coordinated by oxygen. The vertex-sharing tetrahedra form a three-dimensional network closely related to that of SiO_2 in the low-cristobalite (α-cristobalite) modification [10, 11]. Structural parameters as refined on the basis of X-ray powder data using Rietveld-methods resulted in slightly smaller lattice parameters with a = 434.14(3) pm, c = 663.7(1) pm [12]. A quartz-analogue modification of boron phosphate can be obtained at pressures above 4 GPa and temperatures above 300 K [13−15].

Alternative syntheses of BPO_4 using triethylborate and phosphoric acid [16] or triethylphosphate and boron trichloride [17] in a sol-gel process have been presented. As boron phosphate has manifested itself as an effective catalyst in several organic reactions such as hydration [18−20], oligomerization [21, 22] and alkylation [23], there is an increasing interest in its heterogeneous catalytic properties. In order to tailor the surface properties of BPO_4, new preparation methods and deposition techniques [24, 25] have

* PD Dr. Ulrich Schwarz
Max-Planck-Institut für Chemische Physik fester Stoffe
Nöthnitzer Str. 40
D-01187 Dresden
Germany
e-mail: schwarz@cpfs.mpg.de

 DOI: 10.1002/zaac.200400002

been developed. Alkylated borate and phosphate precursors have been used to produce boron phosphate catalysts [26−28] with a high specific surface and in order to allow for deposition of BPO_4 on metal substrates or silicate carriers with chemical vapour deposition methods. More recently lithium doped BPO_4 ceramics revealed Li^+-Ion conductivity and have been investigated for their application as solid electrolytes in rechargeable batteries [29−32]. Approaches using hydrothermal procedures have been performed by conventional [10] and microwave techniques [33].

Investigations on multinary borophosphates were initiated only a few years ago which is quite remarkable since the existence of this type of compounds was known for a long time in form of the minerals Lüneburgite [34−37] and Seamanite [38−40], $Mg_3(H_2O)_6[B_2(OH)_6(PO_4)_2]$ and $(Mn_3(OH)_2[B(OH)_4][PO_4]$, respectively. Moreover, early reports on phosphorus compounds explicitly assumed a formation of a quasi-ternary sodium salt of these combined oxo-acids [41]. The syntheses and characterization of a number of borophosphates in systems $M_xO_y - B_2O_3 - P_2O_5$ ($- H_2O$) [M = main group or 3d transition metal] initiated the development of a classification scheme based on linking principles similar to those employed in silicate crystal chemistry. Thus, the multinary compounds can be categorized according to dimensionality of the anionic partial structures, water content of the compounds, and molar B:P ratio of the borophosphate anions [42].

In the context of investigating optical properties motivated by potential applications in non-linear optics, vibrational spectroscopy has proven to be a suitable tool for the characterization of different phases and the determination of certain molecular species present in borophosphate host frameworks [43]. However, progress concerning the interpretation of optical and vibrational properties is hampered by the low symmetry and the large unit cells of the majority of these phases. Thus, we decided to study tetragonal BPO_4 with the aim to determine the necessary parameters for sound analyses of vibration spectra of the more complex compounds. Here, we report results of chemical transport and hydrothermal growth experiments, single crystal structure refinements as well as investigations by means of difference thermal analysis (DTA), thermogravimetry (TG) and vibrational spectroscopy (IR, Raman).

Experimental Section

Ethanol and 2-propanol were used for solvothermal experiments in the system $H_3BO_3 - H_3PO_4$ since attempts in aqueous, cation-free media merely led to micro- or polycrystalline products. The investigations were performed using five different temperatures in the range between 413 K and 523 K for equimolar suspensions of 1.000 g (16.2 mmol) boric acid (Roth, 99.9 %) and 1.865 g (16.2 mmol) ortho-phosphoric acid (Merck, 85 %, p.a.) in ethanol (Roth, 99.8 %). Evaluation of experiments with an initial 1:1 molar composition by means of IR spectroscopy revealed that a number of products contain H_3BO_3 as an impurity phase. Thus, a series of reactions was carried out using an excess of phosphoric acid up to a ratio of 1:2. In all syntheses, the fill factor of the 20 ml Teflon lined steel autoclaves was adjusted to 50 % − 60 %. For reactions carried out at lower temperatures (413 K, 443 K) the autoclaves were positioned horizontally in a commercially available chamber oven, at higher temperatures (473 K, 493 K, 523 K) they were arranged vertically by means of a metal-block or by using an appropriate tube-furnace. After a reaction time of a minimum of two weeks the raw products were filtrated, washed with hot water and diethyl ether and dried in air at 333 K for 72 h.

Chemical transport reaction properties of BPO_4 were investigated using 20 mg of the transport media I_2, PCl_5, or I_2/P mixtures and typically 1 g of BPO_4. For these growth experiments which lasted usually a week, micro-crystalline powders of BPO_4 were placed in evacuated quartz ampoules (100 mm x 16 mm) and transported endothermically from T_2 to T_1 with ΔT = 100 K for T_2 between 1223 K and 1023 K. Using PCl_5 as a transport agent at T_2 = 1073 K, the resulting crystals of BPO_4 showed a pronounced tendency of intergrowth. In order to avoid crystal growth on the surface of the quartz ampoule, deposition of BPO_4 crystals was finally realized on glassy carbon targets.

Difference thermal analysis (DTA) and thermogravimetry (TG) experiments were performed by means of a simultaneous analyzer (STA 409, Netzsch, Al_2O_3 crucibles, thermocouple, heating/cooling rate 10 K/min). Measurements were conducted in an argon atmosphere (Messer-Griesheim, 99.999 %, additionally purified by passing over zeolite molecular sieve, Roth 3 Å, and BTS-catalyst, Merck, gas flow 0.1 l/min) employing an experimental correction for buoyancy.

Infrared spectra were recorded using a Bruker fourier transform spectrometer IFS 66 equipped with a glowbar and a DTGS detector. Typical sample preparations contained 150 mg KBr and 0.8 mg BPO_4. The Raman measurements were performed with a LabRam System 010 (Jobin Yvon) in backscattering mode. For better low-frequency performance, the setup was equipped with additional filters and used the He-Ne 633 nm line with 15 mW as excitation source. The powder sample is placed on a table with motorized drives in the horizontal directions x as well as y and is imaged by means of a microscope objective with a magnification of 50×. To avoid any damage of the sample surface and, therefore, possible decomposition, the beam is attenuated by using optical filters to one third of the laser power. In order to reduce the full width at half maximum of the modes, the samples were cooled down to 83 K in a Linkam THMS 600 temperature stage.

Results and Discussion

Crystal growth

In the solvothermal growth experiments, the alcoholic medium actually consists of a mixture of ethanol and water due to the use of 85 % aqueous H_3PO_4. The solution is likely to contain partially or fully alkylated borate species according to

$$B(OH)_3 + x\ EtOH \rightarrow B(OH)_{3-x}(OEt)_x + x\ H_2O,\ x \leq 3$$

whereas the alkylation of the phosphoric acid is suppressed by the water content of the solution [44].

BPO_4 is formed in the whole investigated temperature range (413 K to 523 K) as evidenced by X-ray powder diffraction data. Visual inspection of the samples by means

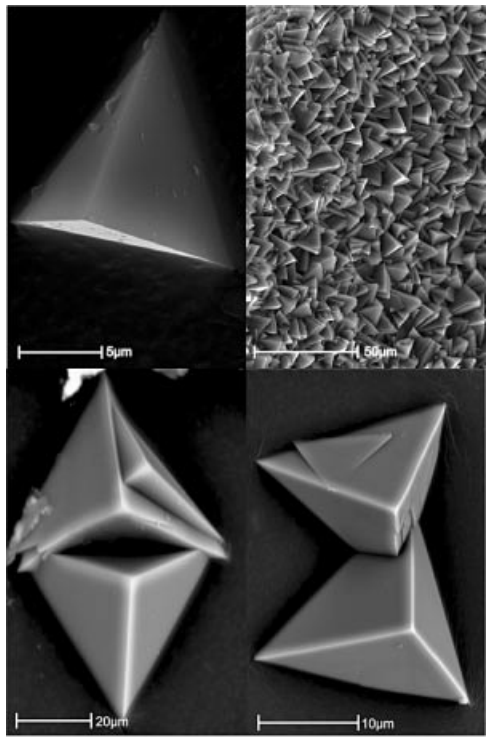

Fig. 1 Scanning electron microscopic image of BPO_4 samples synthesized by solvothermal reaction. Upper left: Tetragonal-bisphenoidic single crystal produced from H_3BO_3 and H_3PO_4 in 2-propanol. Upper right: Layer of BPO_4 crystals as grown on the inner walls of the autoclave. Lower left and right: Particles showing intergrowth and a morphology which is typical for solvothermally grown individuals.

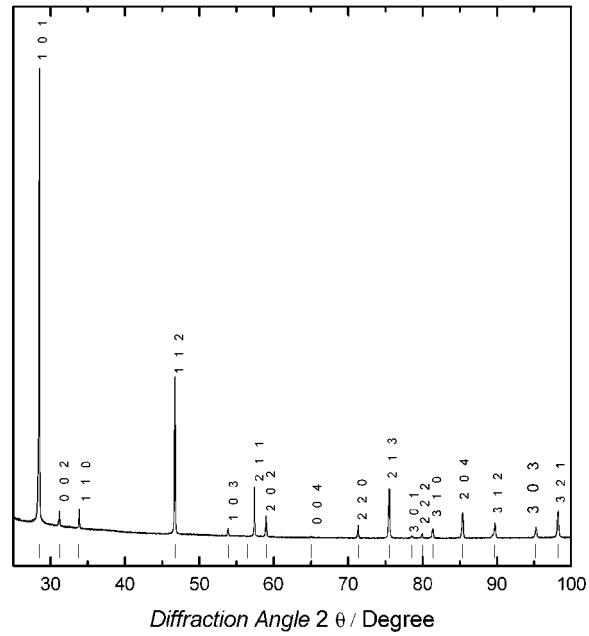

Fig. 2 X-ray powder diffraction pattern (Co$K\alpha_1$) of a purified BPO_4 sample grown by solvothermal reaction (see experimental section). The diffraction diagram can be indexed completely using a tetragonal unit cell which is compatible with the earlier reported lattice parameters. The diagram bears no evidence for the presence of a second crystalline phase.

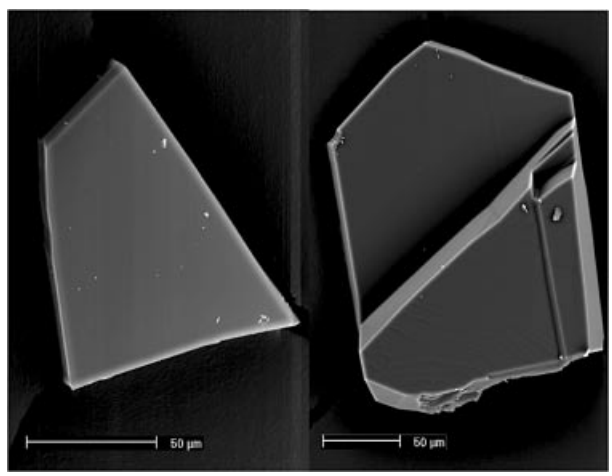

Fig. 3 Scanning electron microscopic image of BPO_4 particles grown by chemical transport reaction. Left: Fragment of a platy individual. Right: Individual showing an intergrowth which is characteristic for samples of BPO_4 grown by CTR.

of optical microscopy reveals that the crystal size strongly depends on the growth temperature. High temperatures (523 K) lead to the formation of micro-crystalline boron phosphate while a lower temperature, e.g., 443 K results in the formation of particles with typical sizes ranging from 10 μm to 20 μm and a higher yield. After a growth period of two weeks at this temperature, a few colourless individuals of BPO_4 with a tetragonal-bisphenoidical shape (Fig. 1) and with sizes sufficient for single crystal Raman and X-ray measurements were obtained. However, the morphology of the crystals clearly reveals that most particles are intergrown. After grinding followed by washing the samples with an excess of hot water (353 K), X-ray powder diffraction data (Fig. 2) bear no evidence for the presence of a second crystalline phase. Peak positions which are indexed by automatic procedures [45−47] and refined lattice parameters are in good agreement with those reported earlier [9, 12].

As an alternative method to grow single crystals we investigated chemical transport reactions (CTR) since earlier experiments indicated that this method is a useful tool in synthesis and crystal growth even of complex oxo-compounds [48−50]. Usually, elemental halogens or halides like NH_4X and HgX_2 (X = Cl, Br, I) are used as transport agents. Alternatively, mixtures of phosphorus and halogen P/X_2 can be utilized as additives.

Using PCl_5 as a transport agent at T_2 = 1073 K and T_1 = 973 K for t = 170 h yielded colourless and fully transparent brick-shaped particles of BPO_4 as well as intergrown particles (Fig. 3). In order to gain deeper insight into the transport reactions and the participating species, we performed

Table 1 Thermodynamic data [51] of phosphates and oxides which have been used for an estimation of $\Delta H(BPO_4, s, 298\ K)$.

$\Delta H°(AlPO_4, s, 298\ K)$	− 1733.431 kJ/mol
$\Delta H°(FePO_4, s, 298\ K)$	− 1297.040 kJ/mol
$\Delta H°(Al_2O_3, s, 298\ K)$	− 1675.692 kJ/mol
$\Delta H°(Fe_2O_3, s, 298\ K)$	− 825.503 kJ/mol
$\Delta H°(P_4O_{10}, s, 298\ K)$	− 3009.936 kJ/mol

an analysis by means of thermodynamic data. The calculation of the standard enthalpy of formation and the free enthalpy for BPO_4 (MPO_4) is based on the values given in Tab. 1. Using these data we obtain for the reaction

$$2\ Al_2O_3\ (s) + P_4O_{10}\ (s) \rightarrow 4\ AlPO_4\ (s)$$

a value of $\Delta H_{R,\ 298\ K} = -572.404$ kJ/mol and in analogy for

$$2\ Fe_2O_3\ (s) + P_4O_{10}\ (s) \rightarrow 4\ FePO_4\ (s)$$

$\Delta H_{R,\ 298\ K} = -527.184$ kJ/mol
is calculated. Thus, the averaged reaction enthalpies amount to
$\Delta H_{R,\ 298\ K} = -549.794$ kJ/mol and
$\Delta H°(B_2O_3, s, 298\ K) = -1271.936$ kJ/mol [51].

Correspondingly, we can estimate for the reaction

$$2\ B_2O_3\ (s) + P_4O_{10}\ (s) \rightarrow 4\ BPO_4\ (s)$$

a standard enthalpy of formation of
$\Delta H°(BPO_4, s, 298\ K) = -1525.9$ kJ/mol
By taking into account that
$S°(BPO_4, s, 298\ K) = 62.383$ J/(mol K) [52] and
C_P (BPO4, s, 700 K) = 139.383 J/(mol K)
we obtain
$\Delta H°(BPO_4, s, 1100\ K) = -1413.765$ kJ/mol
$S°(BPO_4, s, 1100\ K) = 244.997$ J/(mol K)
$\Delta G°(BPO_4, s, 1100\ K) = -1683.253$ kJ/mol.

Thus, we achieve the data which are necessary to describe the transport reaction thermodynamically.
A series of earlier investigations concerning the chemical transport of phosphates with chlorine [50] indicated that P_4O_{10} (g) is the main phosphorus containing transport species in the gas phase. Further thermodynamic calculations evidence [50] that the contribution of mixed species like $POCl_3$ (g) or PO_2Cl (g) [53] to the transport of phosphates is not significant since the ratio $p(P_4O_{10})$ to $p(POCl_3)$ for $p(P_4O_{10}) = p(Cl_2) = 10^5$ Pa at 1273 K corresponds to 278:1. Thus, the relevant transport reaction for phosphates with composition MPO_4 corresponds to

$$4\ MPO_4\ (f) + 6\ Cl_2\ (g) = 4\ MCl_3\ (g) + P_4O_{10}\ (g) + 3\ O_2\ (g).$$

Table 2 Thermodynamic data relevant for a thermodynamic characterization of the investigated transport equilibrium of boron phosphate [51]. For the calculated values of BPO_4, see text.

$\Delta H°(PCl_5, g, 1100\ K)$	− 273.380 kJ/mol
$S°(PCl_5, g, 1100\ K)$	527.087 J/mol K
$\Delta G°(PCl_5, g, 1100\ K)$	− 853.176 kJ/mol
$\Delta H°(BCl_3, g, 1100\ K)$	− 342.670 kJ/mol
$S°(BCl_3, g, 1100\ K)$	385.908 J/mol K
$\Delta G°(BCl_3, g, 1100\ K)$	− 767.169 kJ/mol
$\Delta H°(P_4O_{10}, g, 1100\ K)$	− 2684.217 kJ/mol
$S°(P_4O_{10}, g, 1100\ K)$	745.276 J/mol K
$\Delta G°(P_4O_{10}, g, 1100\ K)$	− 3504.02 kJ/mol

Taking into account the pronounced stability of BCl_3 (g) against dissociation into BCl_2 (g) or BCl (g), the chemical transport realizes a mechanism according to the equation

$$5\ BPO_4\ (s) + 3\ PCl_5\ (g) = 5\ BCl_3\ (g) + 2\ P_4O_{10}\ (g).$$

The derived data for BPO_4 (Tab. 2) are combined with the values given in Tab. 1 in order to gain quantitative results concerning the characteristic thermodynamic parameters of the transport reaction and result in

$\Delta H_{R,\ 1100\ K} = 807.136$ kJ/mol
$\Delta S_{R,\ 1100\ K} = 613.846$ J/(mol K)
$\Delta G_{R,\ 1100\ K} = 131.638$ kJ/mol.

The free reaction enthalpy is correlated with the equilibrium constant of the transport equation by the expression

$$\Delta G_R = -RT \ln K_P$$

and the calculation adds up to

$$K_p = 5.4 \times 10^{-7}.$$

The large positive value of the reaction enthalpy reflects the experimental finding that the transport is endothermic and reproduces also the transport direction from T_2 to T_1 correctly. In general, an efficient chemical transport requires the reversibility of the participating reactions, the existence of a potential gradient and finally experimental conditions close to the equilibrium. These requirements are usually fulfilled by systems which can be described by independent reaction equations and which are characterized by free reaction enthalpies in a range from −100 kJ/mol to 100 kJ/mol. These conditions seem to be violated by the relatively high value of the free reaction enthalpy for the investigated reaction. For the interrelationship between equilibrium constant and partial pressures of the species we obtain

$$K_p = p^5(BCl_3) \times p^2(P_4O_{10}) \,/\, p^3(PCl_5).$$

Assuming the pressure of the transport medium to correspond to

$$p(PCl_5) = 10^5\ Pa$$

we get for BCl_3 (g) as well as for P_4O_{10} (g) transport relevant partial pressures beyond 1 Pa. Thus, despite a rela-

tively high reaction enthalpy the chemical transport of BPO_4 using PCl_5 appears to be coherent in the light of the thermodynamic data and is appropriately characterized by the specified essential transport equation.

A quantitative analysis of the transport rates was impeded by the reaction of BPO_4 with the SiO_2 of the ampoule material. Qualitatively it is found that the transport rates increase with rising temperatures. In the experiments with iodine or I_2/P mixtures, the results do not evidence transport of significant amounts of BPO_4.

Single crystal structure refinements

The atomic arrangement of BPO_4 was refined by means of X-ray single crystal diffraction data (Tab. 3 − Tab. 5). The observed small differences in lattice parameters (Tab. 3) may be attributed to different real structures of the individuals due to strongly dissimilar growing conditions, i.e., the crystal obtained by chemical transport represents BPO_4 material which is quenched from approximately 1000 K whereas the hydrothermally grown crystals are formed at much lower temperatures. BPO_4 crystallizes in a distorted and ordered superstructure of the low-cristobalite type (Fig. 4) with an axial ratio $c/a = 1.53$ strongly deviating from the value of $\sqrt{2} = 1.41$ for cubic high-cristobalite (β-cristobalite). The $[PO_{4/2}]$ and $[BO_{4/2}]$ polyhedra are connected in an alternating fashion by sharing common vertices thus forming a 3D-infinite network. The resulting angle (B−O−P) of 132.1(1)° is rather large and we would like to point out here that the observed displacement of oxygen is maximal in the direction perpendicular to the plane through the B, O and P atoms (see Tab. 5).

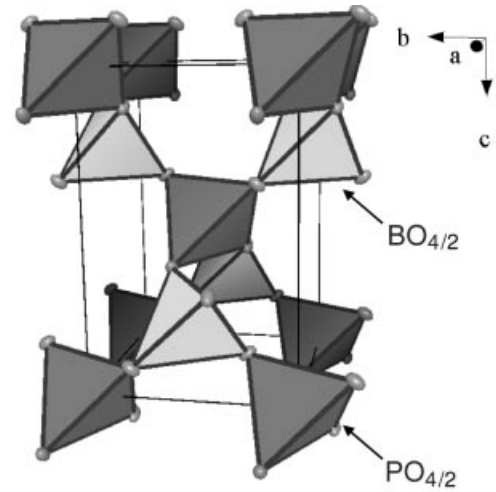

Fig. 4 Crystal structure of BPO_4. The atomic arrangement represents a distorted and ordered superstructure of the low-cristobalite (α-cristobalite) type. The organisation can be described as a 3D network of vertex-sharing $[BO_{4/2}]$ and $[PO_{4/2}]$ tetrahedra. Dark tetrahedra represent $PO_{4/2}$ units, pale ones $BO_{4/2}$.

DTA-TG and infrared spectroscopy

The thermoanalytic investigations of BPO_4 powders reveal that the chemically transported samples show no detectable mass loss between room temperature and 1373 K (Fig. 5). Commercially available microcrystalline powder shows a weight loss at 373 K which is attributed to the evaporation of water as evidenced by results of IR measurements (see Fig. 6 and text below). As-grown material by means of sol-

Table 3 Crystallographic data as well as parameters of intensity data collection and refinement of BPO_4 at ambient conditions ($T = 293$ K). Lattice parameters are determined from X-ray power diffraction data recorded using LaB_6 ($a = 415.69$ pm) as an internal standard.

	Chemical Transport	Hydrothermal growth
Crystal	Prism-shaped fragment 0.14 mm × 0.06 mm × 0.07 mm	Tetragonal bisphenoid 0.035 mm × 0.039 mm × 0.045 mm
Space group	$I\bar{4}$ (No. 82)	$I\bar{4}$ (No. 82)
Formula units per unit cell	$Z = 2$	$Z = 2$
Unit cell	$a = 434.04(1)$ pm $c = 665.02(2)$ pm	$a = 433.79(1)$ pm $c = 665.13(3)$ pm
Volume	$V = 125.284(6) \times 10^6$ pm^3,	$V = 125.16(4) \times 10^6$ pm^3
Calculated density	$\rho = 2.804$ g cm^{-3}	$\rho = 2.807$ g cm^{-3}
Data collection	Rigaku R-AXIS Rapid, Mo K_α, $\lambda = 71.069$ pm, graphite monochromator, 52 images, $\Delta\omega = 5°$, $70° \le \omega \le 130°$, $\chi_1 = 0°$, $\varphi_1 = 0°$, $\chi_2 = 45°$, $\varphi_2 = 90°$	Rigaku AFC7-CCD, Mo K_α, $\lambda = 71.073$ pm, graphite monochromator, 300 images with $\Delta\varphi = 0.8°$, 75 images with $\Delta\omega = 0.8°$.
No. of measured / unique reflections	1484 / 440	475 / 159
R_{eq}	0.032	0.018
Measured range	$2\theta_{max} = 90.18°$ $-8 \le h \le 8$, $-6 \le k \le 8$, $-11 \le l \le 9$,	$2\theta_{max} = 58.76°$ $-4 \le h \le 4$, $-5 \le k \le 4$, $-8 \le l \le 8$,
No. of reflections used for refinement [$F(hkl) > 4\,\sigma F(hkl)$]	428	157
Crystal structure refinement	full matrix least squares on $F^2(hkl)$	full matrix least squares on $F^2(hkl)$
No. of refined parameters; GooF	14; 1.19	14; 1.20
$R(F)$, $wR2$	0.025, 0.057	0.026, 0.055

Table 4 Positional and displacement parameters (in 10^4 pm^2) as well as interatomic distances d(P−O) and d(B−O) for BPO_4 as determined by single crystal structure refinements of individuals which were grown by chemical transport or by hydrothermal synthesis, respectively. Phosphorus is located on Wyckoff position 2*a* (0,0,0), boron on 2*c* (0,1/2,1/4) and oxygen on 8*g* (*x,y,z*).

	Chemical Transport	Hydrothermal Growth
U_{eq} (B)	0.0069(3)	0.0076(9)
U_{eq} (P)	0.0052(1)	0.0083(3)
U_{eq} (O)	0.0081(1)	0.0092(4)
x(O)	0.1405(2)	0.1397(4)
y(O)	0.2579(2)	0.2574(4)
z(O)	0.1271(1)	0.1273(3)
d(B−O) / pm	146.43(7)	146.3(2)
d(P−O) / pm	152.94(7)	152.7(2)

Table 5 Anisotropic displacement parameters U_{ij} / pm^2 of BPO_4 grown by **a)** chemical transport reaction and **b)** solvothermal synthesis, respectively.

a) Atom	U_{11}	U_{22}	U_{33}
B	67(4)	U_{11}	73(8)
P	54(1)	U_{11}	98(3)
O	73(2)	86(2)	83(3)
	U_{23}	U_{13}	U_{12}
O	−32(2)	−1(2)	−1(2)

b) Atom	U_{11}	U_{22}	U_{33}
B	67(14)	U_{11}	93(20)
P	82(4)	U_{11}	86(5)
O	69(8)	113(9)	94(8)
	U_{23}	U_{13}	U_{12}
O	4(6)	4(6)	2(6)

vothermal reactions using an educt ratio H_3BO_3:H_3PO_4 of 1:1 reveals no extra lines in X-ray powder diffraction patterns (see Fig. 2) so that the results would be consistent with pure BPO_4. However, signals of boric acid are clearly discernible in some IR spectra, e.g., at 3220 cm^{-1}, 2260 cm^{-1} and 1473 cm^{-1}. Further investigations of carefully cleaned and dried solvothermal samples grown with educt ratios H_3BO_3:H_3PO_4 ranging from 1:1.5 to 1:2 result in typical weight losses of 1.5 % starting at 560 K. Moreover, they show the onset of a second, more gentle decline at 800 K which amounts to typically −1 %. Thermogravimetry combined with mass spectroscopy unambiguously evidence that the evaporating species of both steps correspond to water. Analyses of X-ray powder diffraction data evidence that heating to 1273 K induces a small, but significant reduction of the full width at half maximum of the diffraction lines, e.g., from 0.1373(7)° to 0.1309(3)°. However, in our investigation the values for unheated samples range from 0.1228(3)° to 0.1359(3)° thus indicating that differences between the individual samples are more pronounced than the effect of heating. Infrared spectra of the as-grown solvothermal material indicate a number of absorptions (Fig. 6) in the frequency range from 3200 cm^{-1} to approximately 3600 cm^{-1}. In agreement with the results from the TG measurements, the feature at 3520 cm^{-1} has been attributed to the presence of H_2O (or OH), that at 3555 cm^{-1} to B−O−H groups which are hydrogen bonded to P−O−H groups, the structure at 3595 cm^{-1} P−O−H groups which are hydrogen bonded to B−O−H species, and the peak at 3635 cm^{-1} to P−O−H units [54−56]. Finally, our experimental data indicate that the pronounced structure at 3230 cm^{-1} also has to be assigned to water. Thus, the experimental IR data are consistent with the TG/MS results both evidencing that the as-grown product contains a significant amount of water as well as protonated borate and phosphate groups which release water upon heating. After grinding and heating the sample to 1273 K with 10 K/min and keeping it in direction of decreasing temperatures at 1073 K for two hours, the extra-lines of the hydrogen-bonded P−O−H and B−O−H groups are no longer visible. The peaks at 3230 cm^{-1} and at 3520 cm^{-1} weaken, but remain clearly discernible. This finding is only compatible with the presence of additional water in form of inclusions. When the dried samples are exposed to air for weeks, water is absorbed as is consistently evidenced in IR and TG experiments by showing an increased intensity of the bands at 3230 cm^{-1} and at 3520 cm^{-1} as well as by exhibiting a weight loss which amounts to approximately − 0.3 % with an onset temperature of 373 K, respectively.

In the context of hydrated species it seems promising to investigate if OH-groups influence the catalytic activity of

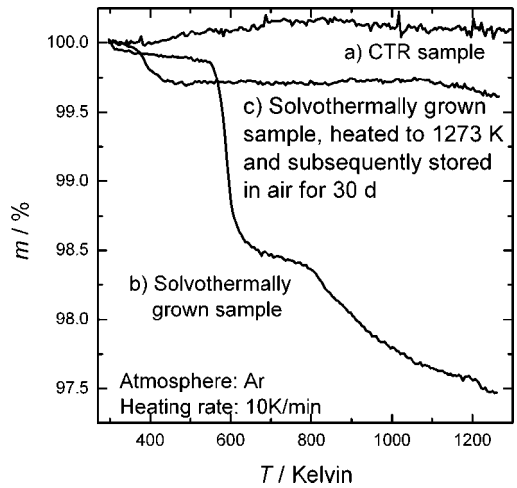

Fig. 5 Thermogravimetric measurements with correction for buoyancy of different BPO_4 powders: **a)** sample grown by chemical transport reaction (CTR) which shows constant mass between room temperature and 1373 K; **b)** desorption of water of a solvothermally-grown sample which was dried at 1373 K and subsequently exposed to air for approximately four weeks; **c)** product grown by solvothermal reaction which shows step-wise weight decrements due to water losses.

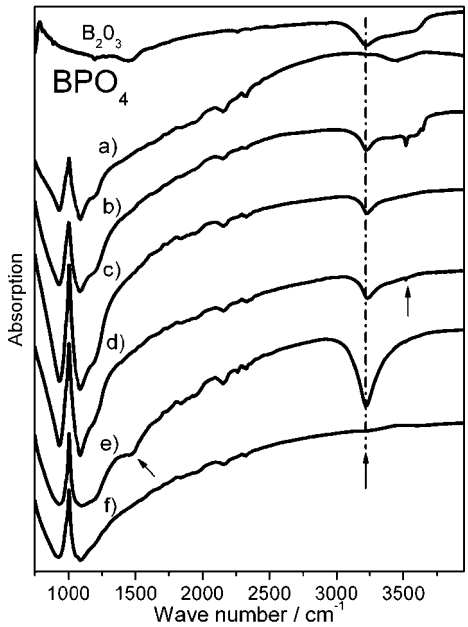

Fig. 6 Infrared spectra of B_2O_3 as a reference and different BPO_4 samples (a − f). Sample **a)** was grown by chemical transport reaction (CTR), samples **b − d)** were synthesized under solvothermal reaction conditions (see experimental section for details): **b)** is as grown, **c)** was subsequently heated up to 1273 K with a rate of 10 K/min, **d)** was exposed to air for one week after the heating; **e)** and **f)** are commercially available powders: **e)** shows a spectrum of the material as delivered, **f)** that of a dried specimen (12 h, 420 K, dynamic vacuum). The weak structures at 3520 cm^{-1} are attributed to water or OH-groups (see text), the strong band at 3230 cm^{-1} (indicated by a dashed-dotted line) to water. The weak peaks in b) between 3500 cm^{-1} and 3600 cm^{-1} indicate hydrogen bonded B−OH and P−OH groups in solvothermally-grown BPO_4.

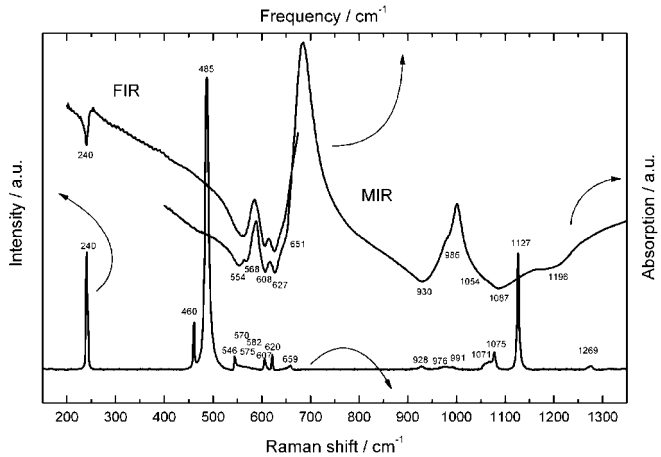

Fig. 7 Spectra in form of intensities (left scale) versus Raman shift (lower scale) measured at 83 K in comparison to room temperature infrared data in form of absorption (right scale) versus frequency (upper scale). For both Raman and IR investigations solvothermally grown BPO_4 has been used.

the material. In an earlier investigation, different activities and selectivities of boron phosphate catalysts in the dehydration and dehydrogenation of alcohols have been observed. However, the disparities have been assigned to the different B:P quotient of the materials originating from different compositions [19] since the focus of the work was to investigate the interdependence of B:P ratio and activity. For solvothermally grown BPO_4, a similar composition dependence is unlikely since the material shows only small variations of the B:P ratio with an average of 1:1.02(1) being close to the ideal molar ratio of 1:1. The quantitative amount of boron present in the sample was determined by means of chemical analysis and indicates that the investigated sample consisted to 96.8 weight percent of BPO_4 which is in good agreement with the observed mass losses in TG ranging from 1.5 % to 3.5 % for different samples.

Raman scattering experiments

Several IR [33, 56−62] and Raman [60, 61, 63, 64] spectra of BPO_4 have been published so far. Concerning the mode assignment, no direct measurements of the mode symmetry have been reported and the modes have been discussed merely in terms of the internal vibrations of the PO_4 and BO_4 tetrahedra.

According to a group theoretical analysis one would expect $6 \times 3 = 18$ vibrations for BPO_4 of which 15 are optically active and 3 are acoustic. The 15 optical vibrations can be grouped by irreducible representations as follows: $\Gamma = 3\ A + 4\ B + 4\ E$, while the three acoustic vibrations are of symmetry B and E, respectively. Concerning the optical modes, all modes are Raman active while only those with symmetry B and E can be observed in IR experiments. To conclude, we expect 8 modes in a powder IR measurement and 11 modes in powder Raman scattering, where the latter number may increase due to LO-TO splittings of the B and E modes. The actuality that more modes are observed in both types of spectra (see Fig. 6 and Fig. 7) is subject of an ongoing theoretical investigation by means of first principles lattice dynamics calculations. An assignment on the basis of these results will be subject of a forthcoming contribution.

Acknowledgement. We are grateful to *Dr. Reiner Ramlau*, *Katja Schulze* and *Petra Scheppan* for electron microscopical investigations. We thank *Dr. Gudrun Auffermann* and *Anja Völzke* for supporting our work by performing a number of chemical analyses, *Dr. Rainer Niewa* and *Susann Müller* for DTA, DSC and TG measurements, and *Dr. Peer Schmidt* and *Hannelore Dallmann* (TU Dresden) for TG/MS investigations. Finally, we like to express our sincere thankfulness to *Dr. Werner Marx* (MPI für Festkörperforschung) and *Ina Wanschura* for patiently tracking down essential references.

References

[1] A. Vogel, *Z. Chem.* **1870**, 125.
[2] G. Gustavson, *Z. Chem.* **1871**, *1*, 417.
[3] G. Meyer, *Ber. Dtsch. Chem. Ges.* **1889**, *22*, 2919.

[4] F. Mylius, A. Meusser, *Ber. Dtsch. Chem. Ges.* **1904**, *37*, 397.
[5] M. Levi, L. F. Gilbert, *J. Chem. Soc.* **1927**, 2117.
[6] C. Aschmann jr., *Chem. Ztg.* **1916**, *136*/*137*, 960.
[7] J. Prescher, *Arch. Pharm.* **1904**, *242*, 199.
[8] E. Gruner, *Z. Anorg. Allg. Chem.* **1934**, *219*, 181.
[9] G. E. R. Schulze, *Z. Phys. Chem.* **1934**, *24*, 215.
[10] K. Kosten, H. Arnold, *Z. Kristallogr.* **1980**, *152*, 119.
[11] F. Hund, *Z. Anorg. Allg. Chem.* **1963**, *321*, 1.
[12] B. Albert, *Z. Kristallogr. Suppl.* **2001**, *18*, 151.
[13] F. Dachille, R. Roy, *Z. Kristallogr.* **1959**, *111*, 451.
[14] J. D. Mackenzie, W. L. Roth, R. H. Wentorf, *Acta Crystallogr.* **1959**, *12*, 79.
[15] F. Dachille, L. S. Dent Glasser, *Acta Crystallogr.* **1959**, *12*, 820.
[16] E. Cherbuliez, J.-P. Leber, A.-M. Ulrich, *Helv. Chim. Acta* **1953**, *36*, 910.
[17] W. Gerrard, P. F. Griffey, *Chem. Ind.* **1959**, 55.
[18] M. Ruwet, P. Berteau, S. Ceckiewicz, *Bull. Soc. Chim. Belg.* **1987**, *96*, 283.
[19] J. B. Moffat, *Cat. Rev. Sci. Eng.* **1978**, *18*, 199.
[20] R. Tartarelli, M. Giorgini, A. Lucchesi, G. Stoppato, F. Moreli, *J. Catal.* **1970**, *17*, 41.
[21] Y. Imizu, S. Aoyama, H. Itoh, A. Tada, *Chem. Lett.* **1981**, *10*, 1455.
[22] A. Tada, H. Suzuka, Y. Imizu, *Chem. Lett.* **1987**, *2*, 423.
[23] J. Morey, J. M. Marinas, J. V. Sinisterra, *React. Kinet. Catal. Lett.* **1983**, *22*, 175.
[24] S. Sato, M. Hasegawa, T. Sodesawa, F. Nozaki, *Bull. Chem. Soc. Jpn.* **1991**, *64*, 516.
[25] L. M. Michael, J. T. Boland, *Surf. Coat. Tech.* **1997**, *94*/*95*, 451.
[26] C. Keary, J. B. Moffat, *J. Coloid. Interf. Sci.* **1992**, *154*, 8.
[27] J. B. Moffat, J. F. Neeleman, *J. Catal.* **1973**, *31*, 274.
[28] D. A. Lindquist, S. M. Pointdexter, S. S. Rooke, D. R. Stockdale, K. B. Babb, A. L. Smoot, W. E. Young, *Proc. Arkansas Acad. Sci.* **1994**, *48*, 100.
[29] M. J. G. Jak, E. M. Kelder, Z. A. Kaszkur, J. Pielaszek, J. Schoonman, *Solid State Ionics* **1999**, *119*, 159.
[30] M. J. G. Jak, E. M. Kelder, J. Schoonman, *J. Solid State Chem.* **1999**, *142*, 74.
[31] M. J. G. Jak, E. M. Kelder, J. Schoonman, N. M. van der Pers, A. Weisenburger, *J. Electroceram.* **1998**, *2*, 127.
[32] E. M. Kelder, M. J. G. Jak, F. de Lange, J. Schoonman, *Solid State Ionics* **1996**, *85*, 285.
[33] A. Baykal, M. Kizilyalli, M. Toprak, R. Kniep, *Turk. J. Chem.* **2001**, *25*, 425.
[34] C. Noellner, *Münch. Akad. Ber.* **1870**, 291.
[35] W. Biltz, E. Marcus, *Z. Anorg. Allg. Chem.* **1912**, *77*, 124.
[36] W. Berdesinski, *Naturwissenschaften* **1951**, *38*, 476.
[37] P. K. S. Gupta, G. H. Swihart, R. Dimitrijevic, M. B. Hossain, *Amer. Mineral.* **1991**, *76*, 1400.
[38] E. H. Kraus, W. A. Seaman, C. B. Slawson, *Amer. Mineral.* **1930**, *15*, 220.
[39] E. N. Kurkutova, V. G. Rau, I. M. Rumanova, *Dok. Akad. Nauk SSSR* **1971**, *197*, 1070.
[40] P. B. Moore, S. Ghose, *Amer. Mineral.* **1971**, *56*, 1527.
[41] R. Abegg, *Elemente der dritten Gruppe des periodischen Systems*, S. Hirzel Verlag, Leipzig **1906,** 35.
[42] R. Kniep, H. Engelhardt, C. Hauf, *Chem. Mater.* **1998**, *10*, 2930.
[43] Y. X. Huang, G. Schäfer, W. Carrillo-Cabrera, R. Cardoso, W. Schnelle, J. T. Zhao, R. Kniep, *Chem. Mater.* **2001**, *13*, 4348.
[44] E. Cherbuliez, J.-P. Leber, *Helv. Chim. Acta* **1952**, *35*, 644.
[45] P. E. Werner, L. Eriksson, M. Westdahl, *J. Appl. Cryst.* **1985**, *18*, 367.
[46] A. Boultif, D. Louer, *J. Appl. Cryst.* **1991**, *24*, 987.
[47] D. Louer, M. Louer, *J. Appl. Cryst.* **1972**, *5*, 271.
[48] H. Schäfer, V. P. Orlovskii, M. Wiemeyer, *Z. Anorg. Allg. Chem.* **1972**, *390*, 13.
[49] R. Gruehn, R. Glaum, *Angew. Chem.* **2000**, *112*, 706; *Angew. Chem. Int. Ed.* **2000**, *39*, 692.
[50] R. Glaum, Habilitationsschrift, Univ. Gießen **1999**.
[51] I. Barin, *Thermochemical data of pure substances*, VCH Verlagsgesellschaft mbH, Weinheim **1989**.
[52] V. P. Gluschko, *Termitscheskije Konstanti Weschestw.*, Moskau **1968**.
[53] M. Binnewies, *Z. Anorg. Allg. Chem.* **1983**, *77*, 507.
[54] J. L. Parsons, M. E. Milberg, *J. Am. Ceram. Soc.* **1960**, *43*, 326.
[55] P. Broadhead, A. Newman, *Spec. Chim. Acta* A **1972**, *28*, 1915.
[56] J. B. Moffat, J. F. Neeleman, *J. Catal.* **1974**, *34*, 376.
[57] P. Kmecl, P. Bukovec, *Acta Chim. Slov.* **1999**, *46*, 161.
[58] F. Gesmundo, V. Lorenzelli, *Atti Acad. Nazl. Lincei − Rend. Sci. Fis. Mat. Nat.* **1965**, *38*, 88.
[59] C. E. Weir, R. A. Schroeder, *J. Res. Nat. Bur. Standards A* **1964**, *68*, 465.
[60] A. Adamczyk, M. Handke, *J. Mol. Struct.* **2000**, *555*, 159.
[61] Y. Shi, J. Liang, H. Zhang, Q. Liu, X. Chen, J. Yang, W. Zhuang, G. Rao, *J. Solid State Chem.* **1998**, *135*, 43.
[62] A. A. Kubasov, L. E. Kitaev, *Zh. Prikl. Khim.* **1973**, 212.
[63] W. Dultz, M. Quilichini, J. F. Scott, G. Lehmann, *Phys. Rev. B* **1975**, *11*, 1648.
[64] N. H. Ray, *Phys. Chem. Glasses* **1975**, *16*, 75.

